Transcription Factor FOXK1 Regulates the lncRNA NEAT1 to Promote Glioma Development Through Mediating KDM3A

Feng Liu
Central South University Third Xiangya Hospital
Hao Wu
Central South University Third Xiangya Hospital
Guangyong Wu
Central South University Third Xiangya Hospital
Jun Long
Central South University Third Xiangya Hospital
Jin Dai
Central South University Third Xiangya Hospital
Zhifei Wang (Wang_zhf0316@163.com)
Central South University Third Xiangya Hospital https://orcid.org/0000-0003-2437-3189

Primary research

Keywords: Glioma, NEAT1, miR-128, KDM3A, transcription factor

Posted Date: July 17th, 2020

DOI: https://doi.org/10.21203/rs.3.rs-43514/v1

Abstract

Background: Long noncoding RNAs are widely studied in glioma. However, the role of the lncRNA NEAT1 and KDM3A in glioma has not yet been reported. We aimed to reveal the role of these two lncRNAs in the development of glioma through this study.

Methods: Samples from glioma patients and normal brain tissues were collected, and the expression of NEAT1 was detected by qRT-PCR. A dual-luciferase reporter gene assay, chromatin immunoprecipitation (ChIP), RNA-binding protein immunoprecipitation (RIP), and RNA pulldown experiments were used to identify the relationship between FOXK1, NEAT1, miR-128, and KDM3A. The CCK8 assay, Transwell assay and flow cytometry were used to detect cell viability, invasion and migration ability, and the cell cycle and apoptosis, respectively. Tumor formation experiments verified the effect of NEAT1 on gliomas in vivo.

Results: FOXK1 and NEAT1 were significantly overexpressed in glioma tissues and cells, and NEAT1 was significantly related to WHO classification. FOXK1 bound the NEAT1 gene promoter region in glioma cells, and interference with FOXK1 inhibited NEAT1 expression. NEAT1 inhibited miR-128 expression by binding miR-128; significantly improved cell viability and invasion and migration capabilities; increased the expression of KDM3A and activated the Wnt signaling pathway. Interference with KDM3A reversed the above results. In addition, interference with NEAT1 decreased KDM3A expression and inhibited tumor growth.

Conclusion: Interference with NEAT1 promoted the expression of miR-128, thereby suppressing the expression of KDM3A and inhibiting the occurrence and development of glioma, while the expression of NEAT1 was shown to be regulated by the upstream transcription factor FOXK1.

Background

Glioma, a serious neurological tumor, accounts for more than 70% of primary malignant brain tumors [1]. According to the 2016 edition of the Pathological Classification of Central Nervous System Tumors [2], gliomas are divided into grade – IV gliomas. The more severe the glioma is, the higher the level of its malignancy. Thus far, exposure to ionizing radiation is the only known risk factor for malignant gliomas [3]. For the most serious tumors of the nervous system, the current common treatment methods are surgery [4], chemotherapy [5], targeted therapy [6], and immunotherapy [7]. Despite these various treatment methods, the treatment effect and quality of life of glioma patients remain poor [8]. Therefore, the need to understand the mechanism of glioma to propose effective treatment methods is urgent.

Long noncoding RNAs (lncRNAs) are a group of RNAs that are longer than 200 nt. Many lncRNAs have been studied in gliomas, such as TUG1 [9], MALAT1 [10], and H19 [11]. Nuclear-enriched abundant transcript 1 (NEAT1) is a new lncRNA that is specifically located in nuclear paraspeckles and irregular compartments found in the internuclear chromatin space [12]. NEAT1 is highly expressed in many malignant tumors but downregulated in nonsolid tumors. Many studies on non-small cell lung cancer have reported that NEAT1 functions as an oncogene by competing for binding with microRNAs such as

miR-377 and let-7a [13, 14]. NEAT1 was also demonstrated to be upregulated in laryngeal squamous cell carcinoma and esophageal squamous cell carcinoma and correlated with clinical stage and lymph node metastasis in these two diseases [15, 16]. The oncogenic role of NEAT1 was also demonstrated in colorectal cancer [17], hepatocellular cancer [18], breast cancer [19], ovarian cancer [20] and prostate cancer [21]. However, in acute promyelocytic leukemia (APL), NEAT1 downregulation contributed to the blockade of differentiation in APL [22].

NEAT1 has been shown to be highly expressed in gliomas, and its high expression is a risk factor for the prognosis of glioma patients [23]. At the same time, we found that in atherosclerosis induced by oxidized low-density lipoprotein (ox-LDL), NEAT1 participates in the inflammatory response and oxidative stress through competing with miR-128 [24]. MiR-128 has been confirmed to inhibit glioma cell proliferation and differentiation and promote glioma cell apoptosis [25, 26]. However, no studies have reported the mechanism and mode of action of NEAT1 and miR-128 in gliomas. Therefore, we hypothesized that NEAT1 and miR-128 affect glioma disease progression by a particular mechanism or by regulating a certain gene. This study used in vivo and in vitro experiments to verify the relationship between NEAT1 and miR-128 and to explore the genes and pathways that NEAT1 and miR-128 may target and regulate. The findings of this study will be helpful to reveal the role of NEAT1 in gliomas.

Materials And Methods

Samples collected

A total of 108 FFPE glioma specimens from surgically resected and pathologically confirmed gliomas were collected from 2016.01-2019.12 in our Department of Neurosurgery. All the patients underwent surgery for the first time had not undergone radiotherapy or chemotherapy before surgery. The patients consisted of 73 males and 35 females, with an average age of 59.2 ± 7.3 years. In addition, 34 normal brain tissues were collected from patients undergoing internal decompression for brain injury as a control.

Cell culture and transfection

The human brain normal glioma cell line HEB and the human glioma cell lines U87, U373, A172, U251 and SHG44 were purchased from the Shanghai Cell Bank of the Chinese Academy of Sciences. The HEB cell line and U87, U373, A172, and U251 glioma cell lines were cultured in DMEM containing 10% fetal bovine serum. SHG44 cells were cultured with RPMI-1640 medium containing 10% fetal bovine serum. All cells were digested with 0.25% trypsin and incubated at 37 ℃ in 5% CO_2 under 95% relative humidity. The cells were digested and sub cultured once every 2–3 days, and cells at the logarithmic growth stage were taken for experiments. The cells were seeded in a six-well plate at a density of 1×10^6/well. When the cell density reached 80%, the cells were transfected with Lipofectamine 2000 (11668-019, Invitrogen, New York, California, USA) according to the manufacturer's instructions. The medium was changed, and cells were incubated at 37 ℃ in a 5% CO2 cell incubator for 6 h before being collected 36–48 h after

transfection. Si-FOXK1, si-NEAT1, miR-128 mimic, mimic NC, si-KDM3A, sh-NC and sh-NEAT1 were chemically synthesized by Shanghai GenePharma.

Dual-luciferase assay

Using the JASPAR (http://jaspar.genereg.net/) and UCSC (http://genome.ucsc.edu/) websites, possible FOXK1-binding sites in the NEAT1 promoter were identified. According to the sites, the corresponding mutant recombinant luciferase reporter gene vectors and FOXK1 expression vector were co-transfected into U87 and SHG44 cells for verification by dual-luciferase reporter experiments. Si-NC and si-FOXK1 were co-transfected to test whether FOXK1 binds the NEAT1 promoter. After 48 h of transfection, cells were collected and lysed, and the luciferase reporter gene activity was detected by a luciferase detection kit (D0010, Solarbio, Beijing, China) and a dual-luciferase reporter gene analysis system (Promega, Madison, WI, USA).

The wild-type (WT) or mutant (MUT) sequences at the 3'UTRs of NEAT1 and KDM3A were synthesized and individually cloned into the pGL3 reporter vector according to the instructions of the luciferase detection kit. Lipofectamine 2000 reagent was used to co-transfect glioma cells with each wild-type or mutant plasmid and vector containing miR-128 mimic or mimic NC. Forty-eight hours after transfection, luciferase activity was detected by dual-luciferase assay. Each experiment was repeated three times.

Chromatin immunoprecipitation (ChIP) experiment

Cells in logarithmic growth phase were incubated in formaldehyde at a final concentration of 1%. The cells were incubated at 37 ℃ for 10 min to crosslink the cells with formaldehyde. Centrifugation was carried out at 4 ℃ and 2000 × g for 5 min. The supernatant was discarded, and SDS lysis buffer was added before sonication. The ultrasonication conditions were 4.5 s of ultrasonication with 9 s intervals for 14 cycles. The sonicated supernatant was centrifuged at 10,000 × g for 10 min at 4 ℃. The supernatant was divided into two tubes; anti-FOXK1 antibody (ab18196, Abcam, UK) was added to one tube, and negative control rabbit IgG (ab172730, Abcam) was added to the other tube, after which the tubes were incubated at 4 ℃ overnight. The next day, protein A agarose/salmon sperm DNA (cat # 16157, Sigma-Aldrich, USA) was added to each tube to precipitate the immune complexes. The supernatant was obtained by centrifugation at 10,000 × g for 5 min at 4 ℃ and removed. Nonspecific complexes were eluted with an eluent and decrosslinked at 65 ℃ overnight. A gel recovery kit (B110092, Sango Biotechnology, Shanghai, China) was used to purify and recover DNA fragments for qPCR to detect the binding of FOXK1 and NEAT1.

RNA pulldown assay

This experiment was performed as described previously [27]. U87 and SHG44 cells were transfected with biotinylated miR-128, biotinylated miR-128 Mut or biotinylated negative control. After culture for 48 h, the cells were incubated with M-280 streptavidin magnetic beads (11205D, Thermo Fisher Scientific, Waltham, Massachusetts, USA). After incubation at 4 ℃ for 3 h, the cells were washed three times with

precooled lysis buffer and once with high-salt buffer (0.1% SDS, 1% Triton X-100, 2 mM EDTA, 20 mM Tris HCl (pH 8.0) and 500 mM NaCl). The purified RNA was used to detect the level of NEAT1.

RNA-binding protein immunoprecipitation (RIP)

RNA immunoprecipitation (RIP) was performed according to the instructions of an Imprint® RNA Immunoprecipitation Kit (RIP-12RXN, Sigma-Aldrich, St. Louis, Missouri, USA). When the glioma cells reached 80–90% confluence, they were completely lysed with RIP lysis buffer. One hundred microliters of the whole-cell extract were incubated with RIP buffer containing magnetic beads bound to anti-Ago2 antibody (HPA058075, Sigma-Aldrich). The kit contained a negative control antibody, normal mouse IgG antibody. Coprecipitated RNA was isolated using TRIzol reagent (TaKaRa), and RNA levels were detected by reverse transcription PCR.

Cell proliferation

Glioma cells in logarithmic growth phase were digested and plated in 96-well plates, with approximately 1×10^4 cells per well. Cell transfection was performed the next day, and cells were cultured for 24 h, 48 h, and 72 h. Ten microliters of CCK-8 solution (C0037, Beyotime) was added, and the cells were placed in an incubator for 2 h, after which the absorbance of each well at 450 nm was detected, and a cell growth curve was drawn.

Cell invasion and migration experiments

ECM gel (E1270, Sigma) was thawed in advance at 4 ℃ and moved to an ice box before the experiment began. ECM gel was diluted in serum-free medium at a ratio of 1:8 to form a working solution on ice. The cultured cells were digested, centrifuged and diluted to 2.5×10^5/ml with serum-free medium. Then, the ECM solution was gently pipetted on ice, and 40 μl of the ECM solution was added to the upper chamber of each well in a Transwell apparatus. The ECM solution was incubated at 37 ℃ for 15 min until the gel solidified. Cell suspension (200 μl) was added to the upper chamber of each well, and 500 μl of medium containing 10% FBS was added to the lower chamber. The samples were incubated at 37 ℃ for a few hours, and excess fluid was aspirated from the upper chamber. The cells were washed twice with PBS and fixed with 5% glutaraldehyde at 4 ℃. A 0.1% crystal violet solution was added, and the cells were stained at room temperature for 0.5 h. The cells were washed twice with PBS, following which cells on the upper surface were wiped off with a cotton ball, and the remaining cells were observed under a microscope.

A pen was used to draw a horizontal line evenly every 1 cm underneath a 6-well plate. Approximately 5×10^5 cells were added to each well. After the cells had been seeded, a 200 μl pipette tip was used to make cell scratches perpendicular to the plate. The old medium was aspirated, and the cells were washed 3 times with PBS. After removing the unadhered cells, serum-free medium was added. The cells were incubated at 37 ℃ in a 5% CO_2 incubator. Photos were taken at 0 h and 48 h. The images were analyzed with Image-Pro Plus 6.0 (Media Cybernetics, USA). The cell migration distance at each time point was calculated as the cell spacing at 0 h - cell spacing at that time.

Cell cycle and apoptosis

Flow cytometry was used to detect the cell cycle and apoptosis. After 48 hours of transfection, the cells in each group were cultured in the dark for 30 minutes with propidium iodide (PI). Cultures were collected, and the cell cycle was analyzed by flow cytometry (FACSCalibur, BD Biosciences, San Jose, CA, USA). Data were evaluated as a percentage distribution of cells in G0/G1, S, and G2/M phases. Cultures were performed according to the instructions of an Annexin V-FITC Apoptosis Detection Kit (C1062M, Beyotime), and apoptosis data were analyzed by flow cytometry [27]. Each experiment was repeated three times.

Tumor formation in rats

Forty-eight healthy Sprague Dawley rats aged 4–5 weeks and weighing 90–110 g were purchased from the Guangdong Medical Experimental Animal Center. U87 and SHG44 cells were randomly divided into groups, and the different groups of cells were divided into the sh-NC and sh-NEAT1 groups. Rats were anesthetized intraperitoneally (30 mg/kg sodium pentobarbital) and fixed on a stereotactic apparatus. The intersection of the coronary suture and the sagittal suture was exposed surgically. At this point, a dental drill with a 1 mm bit was used to drill through the skull, the dura mater was punctured with a 10 L1 microthruster, and the needle tip was retracted by 1 mm. A total of 1×10^5 suspended cells (transfected with sh-NC or sh-NEAT1) were injected. Tumor volume was measured by magnetic resonance imaging (MRI) after 2, 3, 4, and 5 weeks of feeding. Rats in each group were sacrificed, and their brain tissue was collected for subsequent qRT-PCR and immunohistochemistry experiments.

Immunohistochemistry (IHC)

The rat brain tissues were fixed in a 4% paraformaldehyde phosphate buffer solution, embedded in paraffin, sectioned, and then baked in a 50 ℃ incubator for 2 h. The sections were dewaxed with xylene, dehydrated in an alcohol gradient for 2 min at each step, and finally placed into distilled water. The sections were boiled in sodium citrate buffer (10 mM sodium citrate, 0.05% Tween-20, pH 6.0) for 15–20 min, cooled to room temperature, and washed with PBS. Goat serum blocking solution was added and incubated for 20 min to remove excess liquid. Anti-KDM3A primary antibody (ab106456, Abcam) was added and incubated overnight at 4 ℃. After washing with PBS, goat anti-rabbit IgG (ab205718, Abcam) secondary antibody was added, and the cells were incubated at room temperature for 1 h. The cells were washed 3 times with PBS for 3 min each. The signal was developed by incubation with DAB for 5–10 min, following which the cells were redyed with hematoxylin for 2 min, and observed under a microscope after routine dehydration, clearing, and mounting.

qRT-PCR analysis

TRIzol was used to extract total RNA from tissues and cells. 5 μg RNA was used for reverse synthesis to generate cDNA with a Superscript III RT Reverse Transcription Kit (#11752050, ABI Invitrogen). The TaqMan microRNA assay (Thermo Fisher Science) with cDNA as the template was used for qRT-PCR. The

reaction was carried out as follows: 95 ℃ for 2 min, followed by 45 cycles at 95 ℃ for 15 s and 60 ℃ for 45 s. U6 was used as an internal parameter to normalize the results.

qRT-PCR to quantify mRNA was carried out according to the instructions of the TaqMan gene expression assay (Applied Biosystems, Foster City, CA, USA). GAPDH was used as an internal reference. The PCR program was designed as follows: 95 ℃ for 2 min, followed by 40 cycles at 94 ℃ for 20 s, 60 ℃ for 20 s, and 72 ℃ for 30 s. The primer sequences are shown in Table 1. The relative transcription level of each target gene was calculated by the relative quantitative method ($2^{-\triangle\triangle CT}$ method) [28].

Table 1
Sequences for qRT-PCR

Name	Forward (5'-3')	Reverse (5'-3')
FOXK1	CAGTTACCGCTTTGTGCAG	GAATTCTGCCAGCCTTTGTC
NEAT1	ATGCCACAACGCAGATTGAT	CGAGAAACGCACAAGAAGG
U6	GGAACGCTTCACGAATTTG	ATTGGAACGATACAGAGAAGATT
KDM3A	ATGCCCACACAGATCATTCC	CTGCACCAAGAGTCGGTTTT
GAPDH	GGACCTGACCTGCCGTCTAG	GTAGCCCAGGATGCCCTTGA

Western blotting

Total protein was extracted from tissues or cells, and the protein concentration was measured using a BCA kit (Thermo, USA). Polyacrylamide gel electrophoresis of samples containing 30 μg of protein was performed at a constant voltage of 90 V for 30 min and 120 V for 50 min. After electrophoresis was completed, proteins were transferred to a PVDF membrane, and the membrane was blocked with 5% skim milk powder at room temperature for 1 h. The membrane was then incubated with the following antibodies at 4 °C overnight: rabbit anti-FOXK1 polyclonal antibody (ab18196, 1:1000, Abcam), rabbit anti-KDM3A monoclonal antibody (ab106456, 1:100, Abcam), rabbit anti-β-catenin polyclonal antibody (ab16051, 1:500, Abcam), rabbit anti-c-Myc monoclonal antibody (ab32072, 1:1000, Abcam), rabbit anti-cyclinD1 monoclonal antibody (ab16663, 1:200, Abcam), and rabbit anti-β-actin monoclonal antibody (ab179467, 1:5000, Abcam). The membrane was washed 3 times with PBST (PBS buffer containing 0.1% Tween-20). Then, horseradish peroxidase-labeled goat anti-rabbit IgG secondary antibody (ab205718, 1: 2000, Abcam) was added and incubated with the membrane at room temperature for 1 h. The membrane was washed 3 times with PBST buffer. After scanning and development with an optical luminometer (GE, USA), the protein bands were scanned using Image-Pro Plus 6.0 software for grayscale analysis of relative protein expression.

Statistical analysis

The data in this study were analyzed using SPSS 21.0 statistical software (SPSS, Inc., Chicago, IL, USA). Counted data are represented by the number of cases and were analyzed by the chi-square test. Measured data are expressed as the mean ± standard deviation. Comparisons between two groups were

performed using the t-test, comparisons between multiple groups were performed using single-factor analysis of variance, and post hoc tests were performed using Tukey's test. $P < 0.05$ indicates that a difference was statistically significant.

Results

The lncRNA NEAT1 is regulated by the transcription factor foxk1 and overexpressed in glioma

NEAT1 was detected in 108 glioma patient brain tissues and 34 normal brain tissues by qRT-PCR. Compared with its expression in normal brain tissues, NEAT1 expression was significantly higher in glioma patients ($P < 0.05$, Fig. 1A). Based on the median NEAT1 expression, the 108 glioma patients were divided into high expression and low expression groups. By analyzing the expression of NEAT1 and the pathological characteristics of the glioma patients, we found that NEAT1 was correlated with WHO classification [2] but not age, sex, tumor size or preoperative KPS score (Table 2). The expression level of NEAT1 was significantly higher in U87 and SHG44 cells than in HEB cells (Fig. 1B). In addition to the significantly increased expression of NEAT1, FOXK1 was highly expressed in glioma tissues and cells (Fig. 1C). Therefore, we knocked down FOXK1 expression in glioma cells and found that the levels of FOXK1 and NEAT1 were significantly reduced after FOXK1 deactivation ($P < 0.05$, Fig. 1D). To determine whether high NEAT1 expression is regulated by a transcription factor, we used the UCSC and JASPAR websites to predict the regulatory relationship between FOXK1 and NEAT1 and possible FOXK1-binding sites in NEAT1 (Fig. 1E). We individually mutated these binding sites and found that mutation at the 2469 site eliminated the effect of FOXK1 on the luciferase activity of the NEAT1 promoter region (Fig. 1F). Mutation at the 2469 site significantly inhibited the luciferase activity of the NEAT1 promoter region, but the other mutations had no effect (Fig. 1G). Subsequent ChIP experiments also confirmed the binding of FOXK1 and NEAT1 at site 2469 in NEAT1 (Fig. 1H).

Table 2
Relationship between the expression of NEAT1 and the pathological characteristics of glioma patients

Variables	Patient number	NEAT1 levels		p value
		Low(n = 48)	High(n = 60)	
Age(years)				0.272
≥ 60	51	26	25	
< 60	57	22	35	
Gender				0.982
Female	35	16	19	
Male	73	32	41	
Tumor size				0.231
≥ 6 cm	62	24	38	
< 6 cm	46	24	22	
WHO				0.002
□-□	41	28	13	
□-□	67	20	47	
KPS				0.189
< 80	52	27	25	
≥ 80	56	21	35	

Interference with NEAT1 inhibited the proliferation and invasion of glioma cells

To further explore the effects of NEAT1 on glioma cells, we interfered with NEAT1 in the U87 and SHG44 cell lines. The expression of NEAT1 was detected by qRT-PCR, and the results showed that compared with the si-NC group, the si-NEAT1-1 and si-NEAT1-2 groups exhibited significantly reduced NEAT1 expression (Fig. 2A). We chose si-NEAT1-1 because of its more pronounced effect in interfering with NEAT1 for subsequent experiments. Through cell proliferation experiments, we found that cell viability was significantly reduced in the si-NEAT1 group compared to the si-NC group (Fig. 2B). Results of the invasion and cell scratch experiments demonstrated that the ability of the cells to invade and migrate was significantly reduced in the si-NEAT1 group (Fig. 2C). These findings suggest that interference with NEAT1 significantly inhibited the growth and invasion of glioma cells.

NEAT1 regulates the expression of KDM3A by inhibiting miR-128

Studies have shown that NEAT1 is involved in inflammation and oxidative stress through competing with miR-128 in oxidized low-density lipoprotein-induced atherosclerosis [24], while miR-128 inhibits the occurrence of glioma [29]. To further study the mechanism by which NEAT1 regulates glioma cells, we overexpressed and interfered with NEAT1 in U87 and SHG44 cells and then detected the expression of miR-128 by qRT-PCR. The results showed that compared with that in the control group, the expression of miR-128 was significantly increased after NEAT1 knock down, and overexpression of NEAT1 significantly decreased the expression of miR-128 ($P < 0.01$, Fig. 3A). In U87 cells, the binding of NEAT1 and miR-128 was detected by dual-luciferase assay. The results showed that miR-128 mimic significantly inhibited the luciferase activity of WT NEAT1 but had no significant effect on mutant NEAT1 (Fig. 3B). Meanwhile, the RIP assay (Fig. 3C) and an RNA pulldown experiment (Fig. 3D) showed that NEAT1 could bind miR-128.

Through the starBase website, we found that miR-128 is a microRNA shared between NEAT1 and KDM3A. In U87 cells, KDM3A was found to be a target gene of miR-128 (Fig. 3E, F) by dual-luciferase assay and RIP experiments. The expression of miR-128 was significantly higher in the miR-128 group, in which miR-128 was overexpressed, than in the mimic NC group, while the expression of KDM3A was significantly lower (Fig. 3G, H). After co-transfection of si-NEAT1 and miR-128 inhibitor, the expression of miR-128 and KDM3A was detected by qRT-PCR. The results showed that the expression of miR-128 was significantly increased, while that of KDM3A was significantly decreased after NEAT1 interference, but the effects of NEAT1 interference were reversed by miR-128 silencing (Fig. 3I). These results indicated that NEAT1 can inhibit the expression of miR-128 by binding miR-128, thus promoting the expression of KDM3A.

NEAT1 regulates the expression of KDM3A to activate the Wnt pathway to promote the growth of glioma cells

Our previous results demonstrated that NEAT1 promotes KDM3A expression by inhibiting miR-128 expression. Furthermore, we transfected groups of U87 and SHG44 glioma cells and detected the expression of miR-128 and KDM3A by qRT-PCR. The results showed that miR-128 expression was significantly reduced in the miR-128 inhibitor + si-NC group compared with the inhibitor NC + si-NC group, while KDM3A expression was significantly increased ($P < 0.05$). In the inhibitor NC + si-KDM3A group, KDM3A expression was significantly increased, but transfection of miR-128 inhibitor and si-KDM3A reversed the changes in KDM3A expression ($P < 0.05$, Fig. 4A, B). Next, we investigated the viability and invasion and migration capabilities of glioma cells (Fig. 4C-E) and found that miR-128 inhibitor significantly improved cell viability and invasion and migration capabilities, while knocked down KDM3A inhibited these functions and reversed the effect of miR-128 inhibitor.

KDM3A has been reported to activate the Wnt signaling pathway in colorectal cancer to promote cell growth and metastasis [30]. Therefore, we detected the expression of β-catenin, c-Myc, and cyclinD1, Wnt-related proteins, by Western blotting. The results showed that miR-128 inhibitor significantly promoted the

expression of β-catenin, c-Myc and cyclinD1. Following KDM3A interference, the expression of β-catenin, c-Myc and cyclinD1 was reduced, and the effect of miR-128 inhibitor was reversed (Fig. 4F). Since proteins related to the Wnt pathway mainly regulate the cell cycle and apoptosis, the cell cycle and apoptosis in the different transfected groups were detected. We found that interference with KDM3A blocked G2/M phase transition and increased apoptosis (Fig. 4G, H). The above results show that NEAT1 can inhibit the expression of miR-128. Inhibition of miR-128 expression promoted the growth of glioma cells, increased the expression of KDM3A, and then activated the Wnt signaling pathway, alleviating the blockade of G2/M phase and reducing apoptosis. Knocked down KDM3A could alleviate the above phenomena, inhibit cell growth and induce cell apoptosis.

Interference with NEAT1 inhibited tumor formation through KDM3A in glioma cells in vivo

After tumors formed in the rat brain, the tumor volume at various time points was measured by MRI. We found that the tumor volume was significantly reduced in the sh-NEAT1 group compared with the sh-NC group ($P < 0.05$, Fig. 5A). Brain tissue was removed and used to detect the expression of NEAT1 and KDM3A by qRT-PCR, and the expression of KDM3A was detected by IHC. The results showed that compared with that in the sh-NC group, the expression of NEAT1 and KDM3A in the sh-NEAT1 group was significantly reduced (Fig. 5B, C).

Discussion

Glioma is the most common primary tumor in the human brain, with an incidence of 5 per 100,000 [31]. Recently, a study showed that NEAT1 acted as a tumor suppressor by inhibiting proliferation and promoting the apoptosis of glioma cells by downregulating miR-92b and subsequently upregulating DKK3 [32]. In our study, NEAT1 expression was significantly higher in 108 glioma patient tissues than in 34 normal brain tissues. After analyzing the expression of NEAT1 and the pathological characteristics of glioma patients, we found that NEAT1 was correlated with WHO classification. The higher the expression of NEAT1 was, the higher the WHO grade was.

NEAT1 was shown to be overexpressed in the heat shock response and induced by HSF1 in MCF7 and HeLa cells [33]. However, whether HSF1 activation and NEAT1 expression are correlated in cancer remains unknown. From our research, we found that both NEAT1 and FOXK1 were upregulated in glioma cells. Forkhead Box Class K (FOXK) protein 1, an evolutionarily conserved transcription factor, was recently recognized as a key transcriptional regulator in a variety of cancers [34, 35]. Through the UCSC and JASPAR websites, we found four FOXK1-binding sites (1324, 1694, 1767 and 2469) in NEAT1. We individually deleted these sites and confirmed by dual-luciferase assay and ChIP that FOXK1 binds NEAT1 at site 2469. Next, we examined the effect of NEAT1 in glioma cells. The results revealed that NEAT1 acts as an oncogene in glioma. Interference with NEAT1 significantly inhibited the proliferation and invasion of glioma cells.

Based on the relationship between NEAT1 and miR-128 in atherosclerosis and the role of miR-128 in gliomas [24, 29], we investigated the role of these two molecules in glioma. NEAT1 and miR-128 were found to be inversely correlated in glioma, and RIP and RNA pulldown assays verified that NEAT1 can bind miR-128. One of the genes targeted by miR-128 is KDM3A. The starBase database was used to confirm that miR-128 is a shared miRNA between KDM3A and NEAT1. Therefore, we investigated the relationship among the three factors through ChIP, RIP and RNA pulldown experiments. NEAT1 was shown to regulate KDM3A by competing with miR-128 to promote the proliferation and invasion of glioma. In addition, interference with NEAT1 reduced KDM3A levels and inhibited tumor growth in vivo. Similarly, Wu et al. [36] reported that NEAT1 is highly expressed and regulates CDK6 to affect glioma growth through competing with miR-139-5p. In hypoxic-ischemic brain injury, NEAT1 acts as a ceRNA to increase the expression of HOXA1 to reduce brain injury by binding miR-339-5p [37]. KDM3A, a histone demethylase also named JMJD1A, is overexpressed in multiple tumor types and promotes cancer progression. Li et al [38] showed that KDM3A controls the tumorigenic potential of colorectal cancer through Wnt/β-catenin signaling. We detected the relative expression levels of proteins in the Wnt pathway and found that interference with KDM3A reduced the expression of β-catenin, c-Myc and cyclinD1. Inhibition of the Wnt pathway blocked the G2/M phase of the cell cycle and increased apoptosis.

Conclusion

Taken together, these findings provide evidence that the lncRNA NEAT1 is highly expressed in glioma through the regulation by the transcription factor FOXK1. Increased NEAT1 can compete with miR-128 to enhance the expression of KDM3A, followed by activation of the Wnt signaling pathway (Fig. 6). These results may be beneficial in understanding glioma and lay a foundation to exploit novel therapeutic targets and further research.

Abbreviations

ChIP
Chromatin immunoprecipitation; RIP:RNA-binding protein immunoprecipitation; lncRNAs:Long noncoding RNAs; NEAT1:Nuclear-enriched abundant transcript 1; APL:acute promyelocytic leukemia; ox-LDL:oxidized low-density lipoprotein; PI:propidium iodide; MRI:magnetic resonance imaging; IHC:Immunohistochemistry; FOXK1:Forkhead Box Class K protein 1.

Declarations

Ethics approval and consent to participate

This study was approved by the Ethics Committee of The Third Xiangya Hospital of Central South University, and the subjects gave their informed consent. All experimental operations follow international conventions on experimental animal ethics and complied with the relevant national regulations.

Consent for publication

All the authors agree to the publication clause.

Availability of data and materials

All data and materials are fully available without restriction. The data generated or analyzed during this study are included in this published article.

Conflicts of interests

The authors declare that they have no competing interests.

Funding

None.

Authors' contributions

Zhifei Wang made substantial contributions to conception and design. Guangyong Wu, Jun Long, and Jin Dai involved in acquisition of data, analysis, and interpretation of data. Feng Liu and Hao Wu prepared the drafting manuscript. Zhifei Wang gave final approval of the version to be published. All authors have reviewed and approved the final submitted manuscript.

Acknowledgments

Not applicable.

References

1. Xin Y, Zhang W, Mao C, et al. LncRNA LINC01140 Inhibits Glioma Cell Migration and Invasion via Modulation of miR-199a-3p/ZHX1 Axis. OncoTargets therapy. 2020;13:1833–44.
2. Wesseling P, Capper D. WHO 2016 Classification of gliomas. Neuropathology applied neurobiology. 2018;44:139–50.
3. Butowski NA. Epidemiology and diagnosis of brain tumors. Continuum (Minneapolis Minn). 2015;21:301–13.
4. McGirt MJ, Chaichana KL, Gathinji M, et al. Independent association of extent of resection with survival in patients with malignant brain astrocytoma. Journal of neurosurgery. 2009;110:156–62.
5. Hegi ME, Diserens AC, Gorlia T, et al. MGMT gene silencing and benefit from temozolomide in glioblastoma. N Engl J Med. 2005;352:997–1003.
6. Batchelor TT, Reardon DA, de Groot JF, Wick W, Weller M. Antiangiogenic therapy for glioblastoma: current status and future prospects. Clinical cancer research: an official journal of the American Association for Cancer Research. 2014;20:5612–9.

7. Ung N, Yang I. Nanotechnology to augment immunotherapy for the treatment of glioblastoma multiforme. Journal of neuro-oncology. 2015;123:473–81.
8. Osoba D, Brada M, Prados MD, Yung WK. Effect of disease burden on health-related quality of life in patients with malignant gliomas. Neurooncology. 2000;2:221–8.
9. Li J, Zhang M, An G, Ma Q. LncRNA TUG1 acts as a tumor suppressor in human glioma by promoting cell apoptosis. Experimental biology medicine (Maywood NJ). 2016;241:644–9.
10. Ma KX, Wang HJ, Li XR, et al. Long noncoding RNA MALAT1 associates with the malignant status and poor prognosis in glioma. Tumour biology: the journal of the International Society for Oncodevelopmental Biology Medicine. 2015;36:3355–9.
11. Shi Y, Wang Y, Luan W, et al. Long non-coding RNA H19 promotes glioma cell invasion by deriving miR-675. PloS one. 2014;9:e86295.
12. Yu X, Li Z. NEAT1: A novel cancer-related long non-coding RNA. 2017; 50.
13. Zhang J, Li Y, Dong M, Wu D. Long non-coding RNA NEAT1 regulates E2F3 expression by competitively binding to miR-377 in non-small cell lung cancer. Oncology letters. 2017;14:4983–8.
14. Qi L, Liu F, Zhang F, et al. lncRNA NEAT1 competes against let-7a to contribute to non-small cell lung cancer proliferation and metastasis. Biomedicine & pharmacotherapy = Biomedecine & pharmacotherapie. 2018; 103: 1507–1515.
15. Chen X, Kong J, Ma Z, Gao S, Feng X. Up regulation of the long non-coding RNA NEAT1 promotes esophageal squamous cell carcinoma cell progression and correlates with poor prognosis. American journal of cancer research. 2015;5:2808–15.
16. Wang P, Wu T, Zhou H, et al. Long noncoding RNA NEAT1 promotes laryngeal squamous cell cancer through regulating miR-107/CDK6 pathway. Journal of experimental clinical cancer research: CR. 2016;35:22.
17. Li Y, Li Y, Chen W, et al. NEAT expression is associated with tumor recurrence and unfavorable prognosis in colorectal cancer. Oncotarget. 2015;6:27641–50.
18. Guo S, Chen W, Luo Y, et al. Clinical implication of long non-coding RNA NEAT1 expression in hepatocellular carcinoma patients. Int J Clin Exp Pathol. 2015;8:5395–402.
19. Choudhry H, Albukhari A, Morotti M, et al. Tumor hypoxia induces nuclear paraspeckle formation through HIF-2alpha dependent transcriptional activation of NEAT1 leading to cancer cell survival. Oncogene. 2015;34:4546.
20. Kim YS, Hwan JD, Bae S, Bae DH, Shick WA. Identification of differentially expressed genes using an annealing control primer system in stage III serous ovarian carcinoma. BMC Cancer. 2010;10:576.
21. Chakravarty D, Sboner A, Nair SS, et al. The oestrogen receptor alpha-regulated lncRNA NEAT1 is a critical modulator of prostate cancer. Nature communications. 2014;5:5383.
22. Zeng C, Xu Y, Xu L, et al. Inhibition of long non-coding RNA NEAT1 impairs myeloid differentiation in acute promyelocytic leukemia cells. BMC Cancer. 2014;14:693.

23. He C, Jiang B, Ma J, Li Q. Aberrant NEAT1 expression is associated with clinical outcome in high grade glioma patients. APMIS: acta pathologica, microbiologica, et immunologica Scandinavica. 2016; 124: 169–174.
24. Chen DD, Hui LL, Zhang XC, Chang Q. NEAT1 contributes to ox-LDL-induced inflammation and oxidative stress in macrophages through inhibiting miR-128. Journal of cellular biochemistry. 2018: 1–9.
25. Huo L, Wang B, Zheng M, et al. miR-128-3p inhibits glioma cell proliferation and differentiation by targeting NPTX1 through IRS-1/PI3K/AKT signaling pathway. Experimental therapeutic medicine. 2019;17:2921–30.
26. Ye Y, Zhi F, Peng Y, Yang CC. MiR-128 promotes the apoptosis of glioma cells via binding to NEK2. European review for medical and pharmacological sciences. 2018; 22: 8781–8788.
27. Wang SH, Zhang WJ, Wu XC, et al. The lncRNA MALAT1 functions as a competing endogenous RNA to regulate MCL-1 expression by sponging miR-363-3p in gallbladder cancer. J Cell Mol Med. 2016;20:2299–308.
28. Xie M, Ma T, Xue J, et al. The long intergenic non-protein coding RNA 707 promotes proliferation and metastasis of gastric cancer by interacting with mRNA stabilizing protein HuR. Cancer letters. 2019;443:67–79.
29. Zhang Y, Chao T, Li R, et al. MicroRNA-128 inhibits glioma cells proliferation by targeting transcription factor E2F3a. J Mol Med. 2009;87:43–51.
30. Peng K, Su G, Ji J, et al. Histone demethylase JMJD1A promotes colorectal cancer growth and metastasis by enhancing Wnt/beta-catenin signaling. J Biol Chem. 2018;293:10606–19.
31. Wen PY, Macdonald DR, Reardon DA, et al. Updated response assessment criteria for high-grade gliomas: response assessment in neuro-oncology working group. Journal of clinical oncology: official journal of the American Society of Clinical Oncology. 2010;28:1963–72.
32. Liu D, Zou Z, Li G, Pan P, Liang G, Long Noncoding. RNA NEAT1 Suppresses Proliferation and Promotes Apoptosis of Glioma Cells Via Downregulating MiR-92b. Cancer control: journal of the Moffitt Cancer Center. 2020;27:1073274819897977.
33. Lellahi SM, Rosenlund IA, Hedberg A, et al. The long noncoding RNA NEAT1 and nuclear paraspeckles are up-regulated by the transcription factor HSF1 in the heat shock response. J Biol Chem. 2018;293:18965–76.
34. Liu Y, Ding W, Ge H, et al. FOXK transcription factors: Regulation and critical role in cancer. Cancer letters. 2019;458:1–12.
35. Zheng S, Yang L, Zou Y, et al. Long non-coding RNA HUMT hypomethylation promotes lymphangiogenesis and metastasis via activating FOXK1 transcription in triple-negative breast cancer. J Hematol Oncol. 2020;13:17.
36. Wu DM, Wang S, Wen X, et al. Long noncoding RNA nuclear enriched abundant transcript 1 impacts cell proliferation, invasion, and migration of glioma through regulating miR-139-5p/ CDK6. Journal of cellular physiology. 2019;234:5972–87.

37. Zhao J, He L, Yin L. lncRNA NEAT1 Binds to MiR-339-5p to Increase HOXA1 and Alleviate Ischemic Brain Damage in Neonatal Mice. Molecular therapy Nucleic acids. 2020;20:117–27.
38. Li J, Yu B, Deng P, et al. KDM3 epigenetically controls tumorigenic potentials of human colorectal cancer stem cells through Wnt/beta-catenin signalling. Nature communications. 2017;8:15146.

Figures

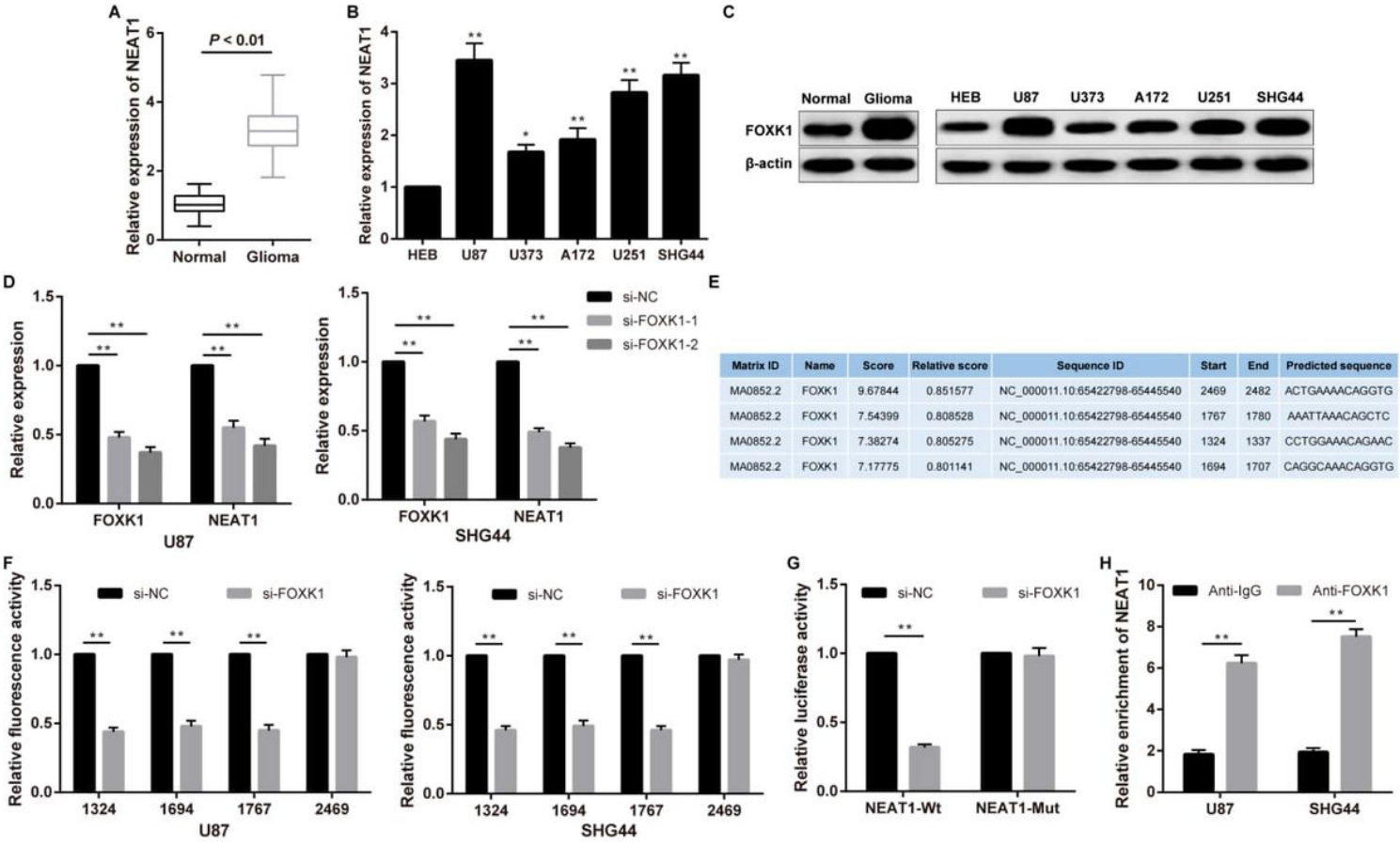

Figure 1

The lncRNA NEAT1 is overexpressed in glioma and regulated by the transcription factor FOXK1. A, NEAT1 expression in glioma tissues (N = 108) and normal brain tissues (N = 34) was detected by qRT-PCR. B, NEAT1 expression in normal human brain normal glial cell lines and human glioma cell lines was detected by qRT-PCR. * indicates P <0.05 compared with HEB cells, ** indicates P <0.01 compared with HEB cells. C, Western blotting was used to detect FOXK1 expression in tissues and cells. D, FOXK1 and NEAT1 expression in glioma cells after interference with FOXK1. ** indicates P <0.01. E, the JASPAR website was used to predict FOXK1-binding sites in the NEAT1 promoter region. F, the specific binding site for FOXK1 in the NEAT1 promoter region was determined by dual-luciferase assay. ** indicates P <0.01. G, the luciferase activity when the 2469 site was mutated is shown. ** indicates P <0.01. H. the ChIP assay was used to detect the binding of FOXK1 and NEAT1. ** indicates P <0.01. The experiment was repeated three times. Data are expressed as the mean ± standard deviation, and a t-test was performed.

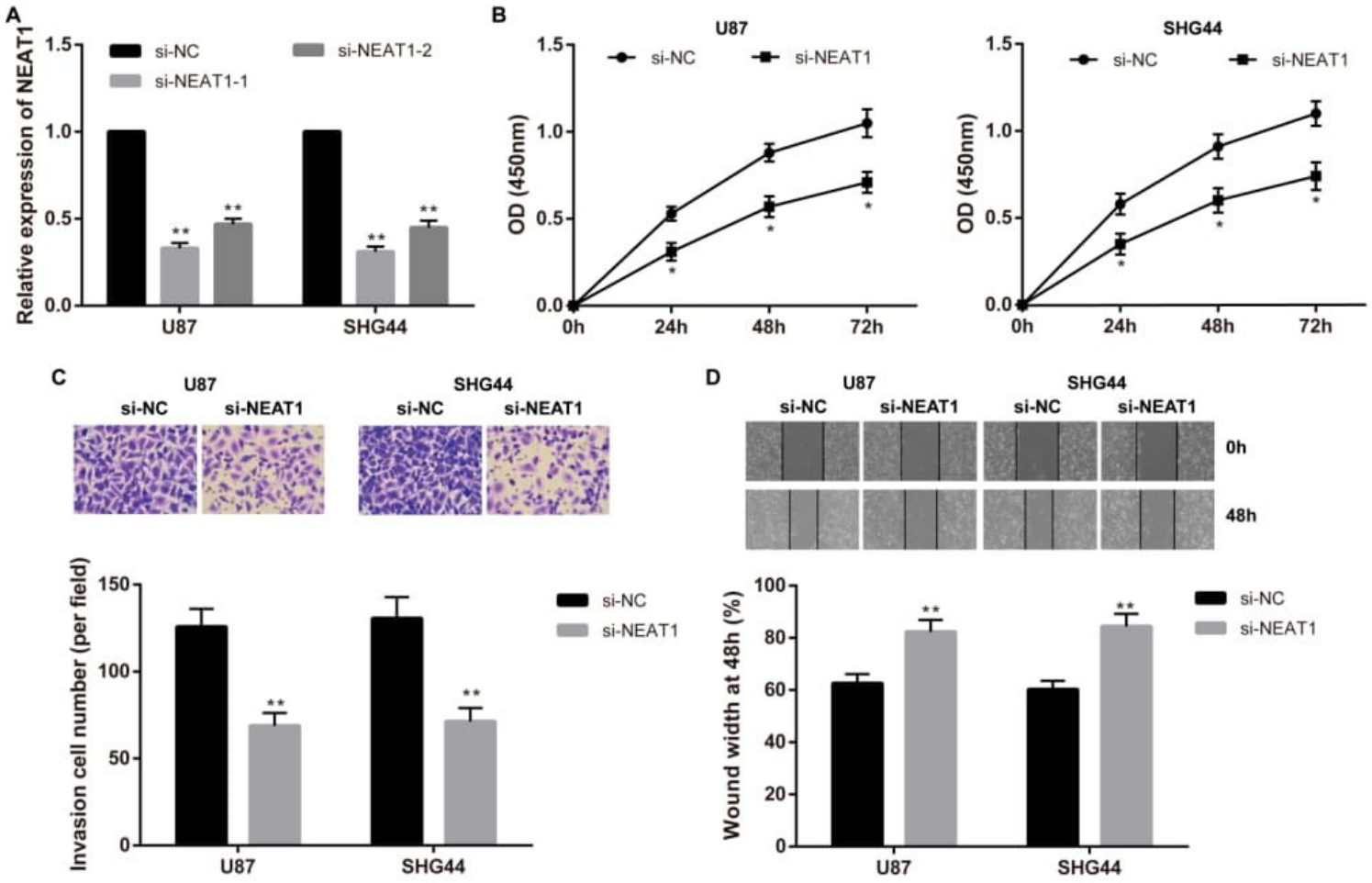

Figure 2

Interference with NEAT1 inhibited glioma cell growth and invasion ability. A, the expression of NEAT1 in U87 and SHG44 cells after NEAT1 interference was detected by qRT-PCR. B, the CCK-8 assay was used to detect the cell viability of U87 and SHG44 cells after interference with NEAT1. C, the Transwell assay was used to detect the invasive abilities of U87 and SHG44 cells after interference with NEAT1 (200×). D, the scratch test was used to detect the migration ability of U87 and SHG44 cells after interference with NEAT1 at 48 h. Each experiment was repeated three times. Data are expressed as the mean ± standard deviation, and a t-test or ANOVA was performed. * indicates P <0.05 compared with the si-NC group, **indicates P < 0.01 compared with the si-NC group.

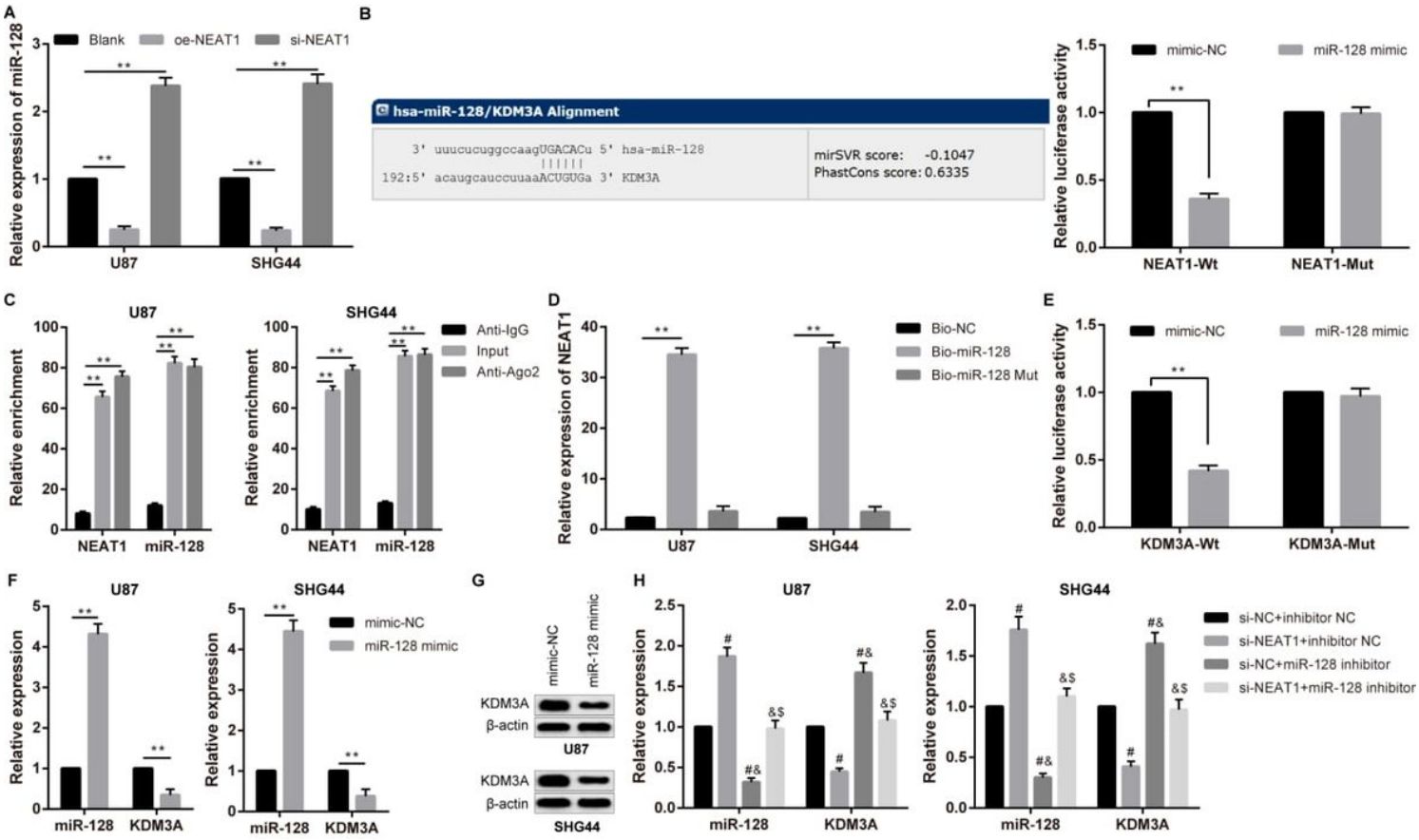

Figure 3

NEAT1 mediates the expression of KDM3A through miR-128. A, miR-128 expression with NEAT1 interference of overexpression is shown. B, a dual-luciferase assay was used to detect NEAT1 and miR-128 binding in U87 cells. C, RIP was used to detect NEAT1 expression. D, an RNA pulldown assay was used to detect NEAT1 and miR-128 binding. E, a dual-luciferase assay was used to detect miR-128 and KDM3A binding in U87 cells. F, RIP was used to detect KDM3A expression in HCT116 cells. G, qRT-PCR was used to detect the expression of miR-128 and KDM3A. H, Western blotting was used to detect the expression of KDM3A. I, qRT-PCR was used to detect the expression of miR-128 and KDM3A. Each experiment was repeated three times. Data are expressed as the mean ± standard deviation, and the t-test or ANOVA was performed. ** indicates P <0.01. # indicates P < 0.05 compared with si-NC+inhibitor NC group. & indicates P < 0.05 compared with si-NEAT1+inhibitor NC group. $ indicates P < 0.05 compared with si-NC+miR-128 inhibitor group.

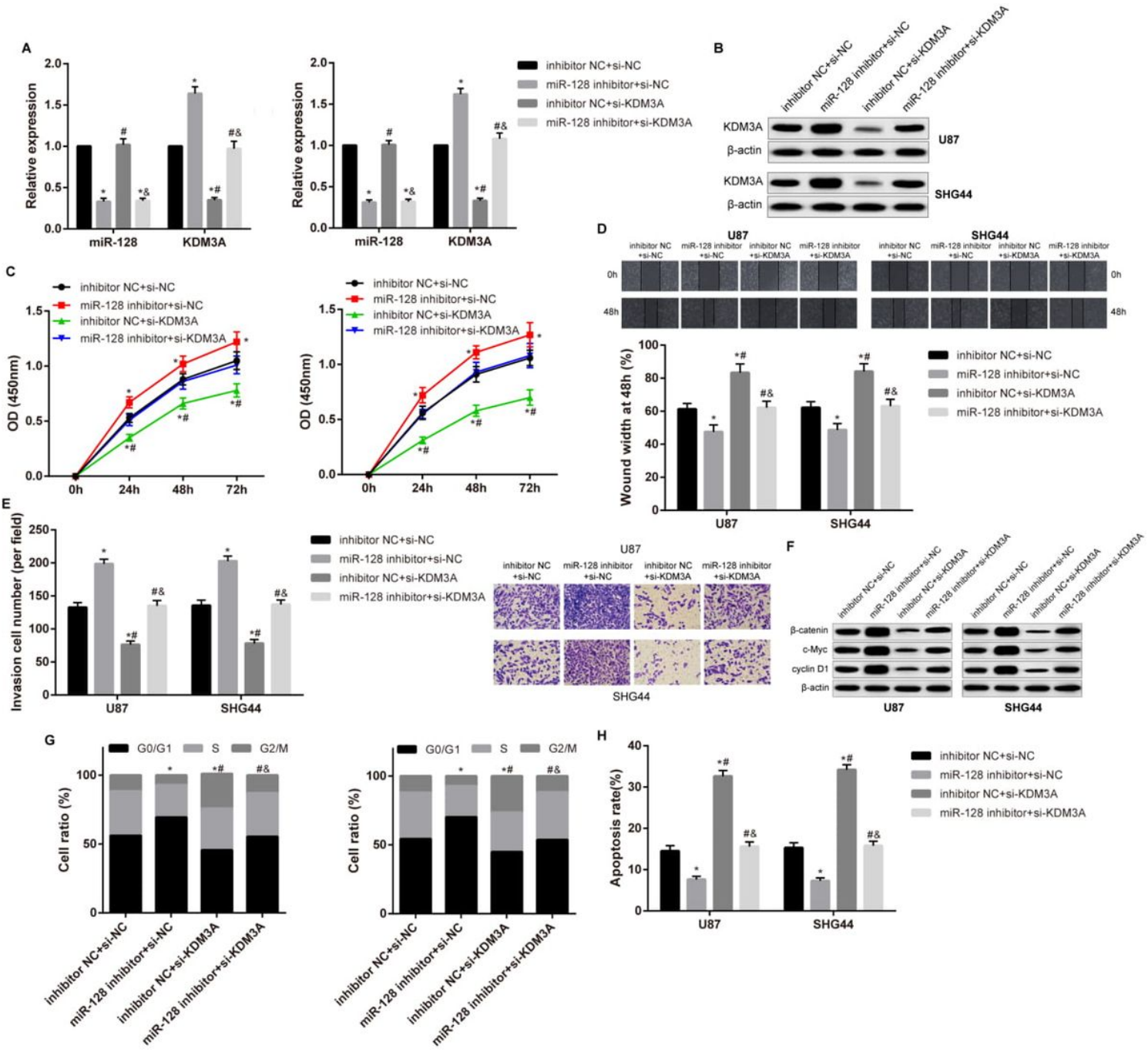

Figure 4

NEAT1 promotes glioma cell growth by activating the Wnt pathway through KDM3A. A, qRT-PCR was used to detect the expression of miR-128 and KDM3A. B, Western blotting was used to detect KDM3A expression. C, the CCK-8 assay was used to detect cell viability in each group. D, the Transwell assay was used to detect cell invasion in each group. E, scratch experiments were used to detect cell migration ability in each group. F, Western blotting was used to detect β-catenin, c-Myc and cyclinD1 expression in each group. G, flow cytometry was used to detect the cell cycle in each group. H, flow cytometry was used to detect apoptosis in each group. Each experiment was repeated three times. Data are expressed as the mean ± standard deviation, and the t-test or ANOVA was performed. * indicates P <0.05 compared with

inhibitor NC+si-NC group. # indicates P < 0.05 compared with miR-128 inhibitor+si-NC group. & indicates P < 0.05 compared with inhibitor NC+si-KDM3A.

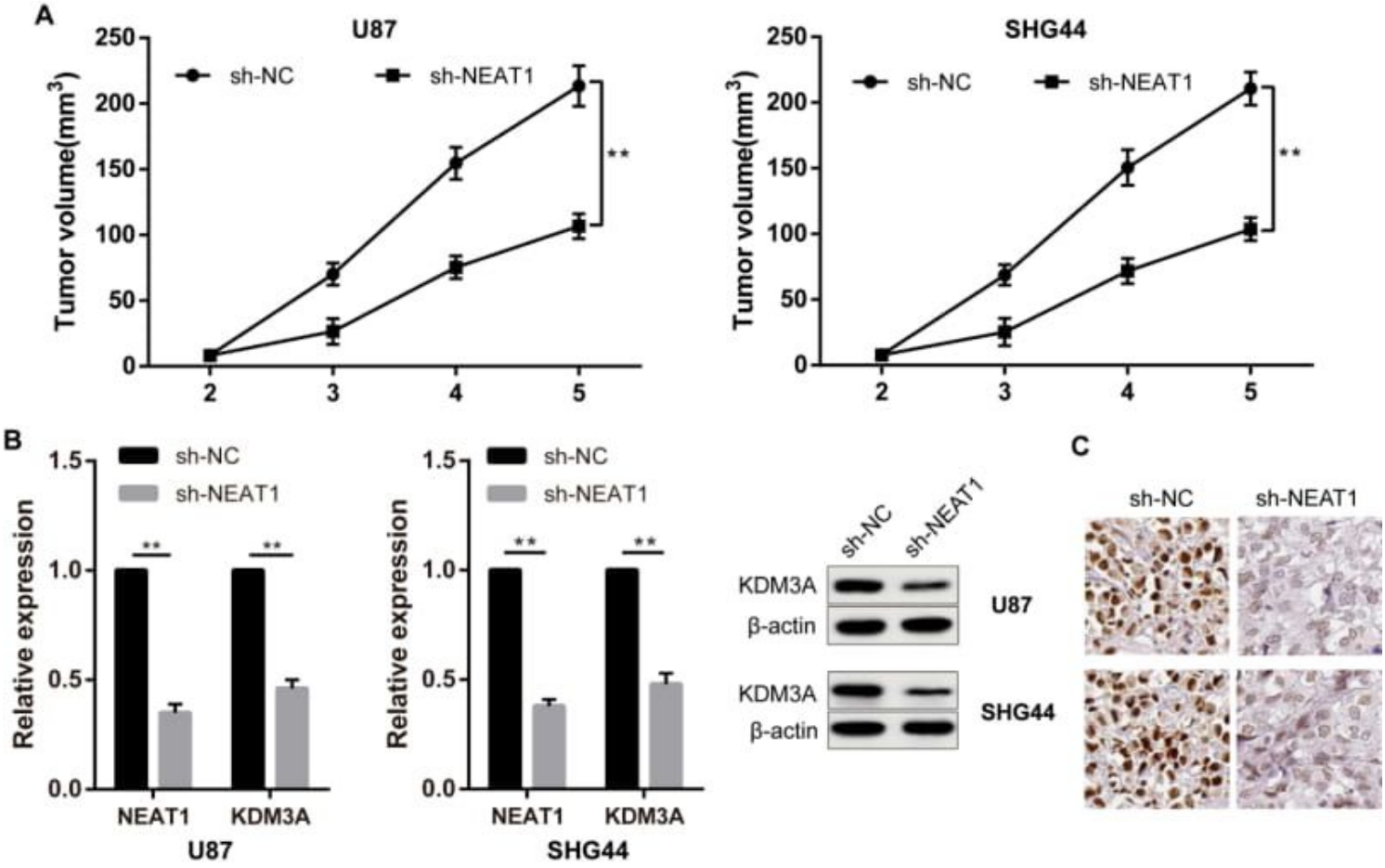

Figure 5

The effects of NEAT1 on glioma cells in vivo. A, the tumor volumes at different time points are shown. B, qRT-PCR was used to detect the expression of NEAT1 and KDM3A. C, IHC was used to detect the expression of KDM3A (×400). ** P < 0.01 compared with the sh-NC group.

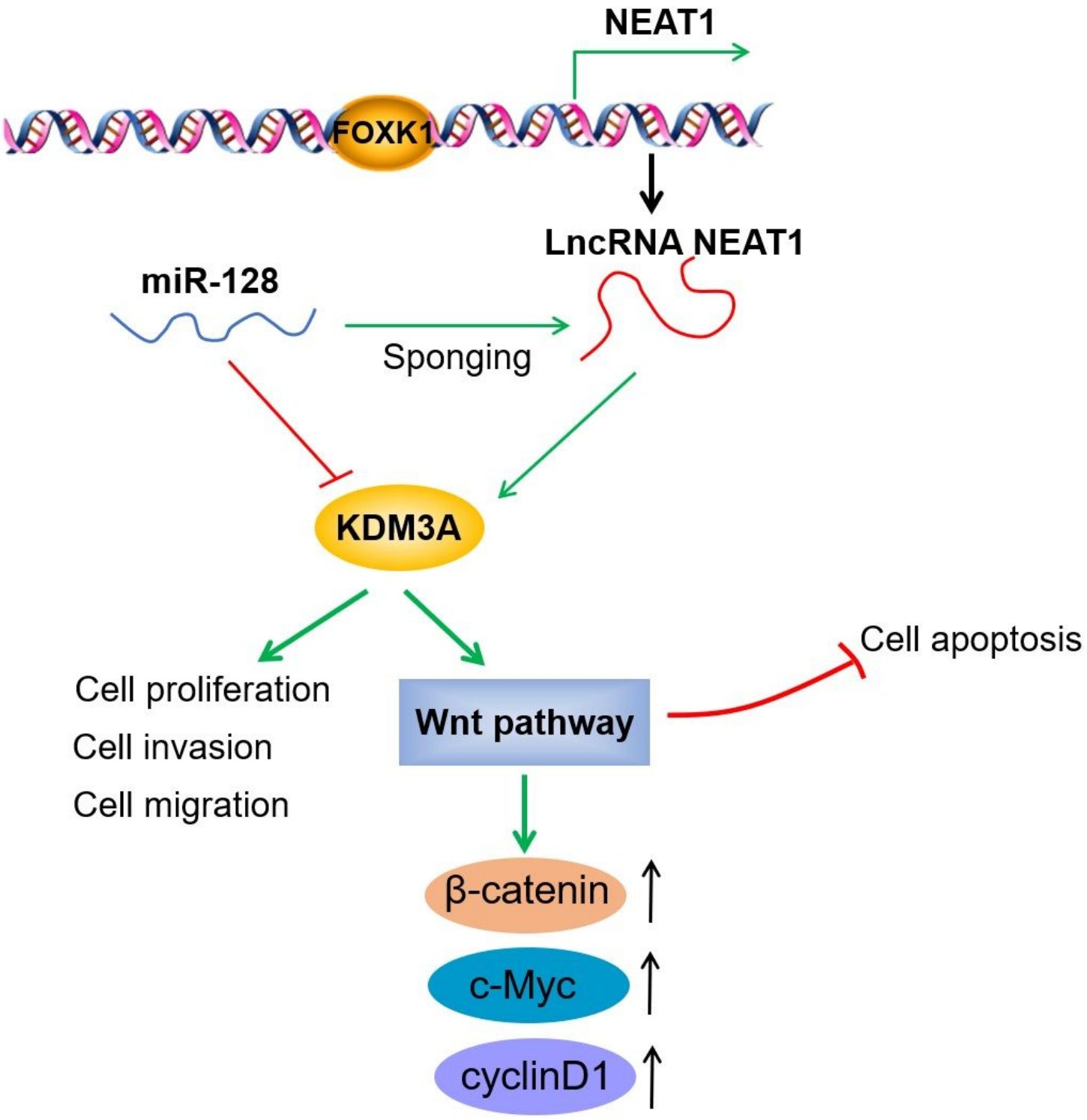

Figure 6

Mechanism diagram illustrating the regulatory network and function of NEAT1, miR-128 and KDM3A in glioma.